

The Early Isoform of Disabled-1 Functions Independently of Reelin-Mediated Tyrosine Phosphorylation in Chick Retina^{∇†}

Zhijua Gao,¹ Elizabeth A. Monckton,¹ Darryl D. Glubrecht,¹ Cairine Logan,² and Roseline Godbout^{1*}

Department of Oncology, University of Alberta, Cross Cancer Institute, 11560 University Avenue, Edmonton, AB T6G 1Z2, Canada,¹ and Department of Cell Biology and Anatomy, University of Calgary, 3330 Hospital Drive NW, Calgary, AB T2N 4N1, Canada²

Received 10 May 2010/Accepted 17 June 2010

The Reelin–Disabled-1 (Dab1) signaling pathway plays a key role in the positioning of neurons during brain development. Two alternatively spliced Dab1 isoforms have been identified in chick retina and brain: Dab1-E, expressed at early stages of development, and Dab1-L (commonly referred to as Dab1), expressed at later developmental stages. The well-studied Dab1-L serves as an adaptor protein linking Reelin signal to its downstream effectors; however, nothing is known regarding the role of Dab1-E. Here we show that Dab1-E is primarily expressed in proliferating retinal progenitor cells whereas Dab1-L is found exclusively in differentiated neuronal cells. In contrast to Dab1-L, which is tyrosine phosphorylated upon Reelin stimulation, Dab1-E is not tyrosine phosphorylated and may function independently of Reelin. Knockdown of Dab1-E in chick retina results in a significant reduction in the number of proliferating cells and promotes ganglion cell differentiation. Our results demonstrate a role for Dab1-E in the maintenance of the retinal progenitor pool and determination of cell fate.

Retinal progenitor cells give rise to six major classes of neurons (cone, rod, bipolar, amacrine, horizontal, and ganglion) and one class of glia (Müller) (31, 60). The temporal birth of retinal cells follows a specific order, with ganglion cells differentiating first, followed by horizontal, amacrine, cone, rod, and then bipolar and Müller glial cells (13). Retinal cells in the mature retina are assembled into three nuclear layers (ganglion, inner, and outer) separated by the inner and outer plexiform layers.

The Reelin–Disabled-1 (Dab1) signaling pathway is a key regulator of neuronal cell positioning. Binding of the extracellular glycoprotein Reelin to its lipoprotein receptors, the very low density lipoprotein receptor (VLDLR) and the apolipoprotein E receptor 2 (ApoER2), activates Src family kinases (SFK) and induces tyrosine phosphorylation of Dab1 (3, 30, 35). The intracellular adaptor protein Dab1 contains three major domains: an N-terminal protein interaction/phosphotyrosine binding (PI/PTB) domain that binds to the NPxY motif within Reelin receptors (59), an internal tyrosine-rich region responsive to Reelin stimulation (43), and a C-terminal serine/threonine-rich region involved in Reelin–Dab1 signaling modulation (29). The tyrosine-rich domain of Dab1 consists of five highly conserved tyrosine residues (Y185, Y198, Y200, Y220, and Y232) that correspond to four tyrosine kinase recognition sites. Y185 and Y198/Y200 are located within two consensus SFK recognition sites (YQXI), whereas Y220 and Y232 are found within two consensus Abl recognition sites (YXVP) (56).

Upon phosphorylation, Dab1 triggers a host of signaling events, including activation of the SFK, phosphatidylinositol 3-kinase (PI-3K)/Akt, mTOR, CrkL/C3G/Rap and LIMK1 (LIM kinase 1) pathways, and phosphorylation of n-cofilin (3, 5, 10–11, 14, 39). Together, these events result in the cytoskeleton remodeling and correct positioning of neurons during development. Dab1 tyrosine phosphorylation is essential for Reelin signaling, since mice expressing the nonphosphorylated Dab1 protein have phenotypes similar to those of mice deficient in Reelin (*reeler*), Dab1 (*yotari/scrambler/Dab1^{-/-}*), or VLDLR and ApoER2 (*VLDLR^{-/-} ApoER2^{-/-}*) (36). These mice exhibit extensive defects in neuronal migration, including layer disruption in the cerebral cortex, cerebellum, and hippocampus (17, 34, 55, 59).

Defects associated with disruption of Reelin–Dab1 signaling are also observed in mouse retina and include a reduction in the number of rod bipolar cells, abnormal synaptic layering of rod bipolar cells, a reduction in the density of AII amacrine dendrites, and alteration in the positioning of amacrine cell processes (53). In humans, *Reelin* mutations are associated with serious ocular and visual abnormalities, including retinal dysplasia and macular hypoplasia (48). In *Drosophila*, inactivation of *Disabled* disrupts ommatidium development and leads to a frequent loss of R7 photoreceptors (46). Thus, Reelin–Dab1 signaling appears to be critical for proper development of the retina as well as the brain.

Alternative splicing of the *Dab1* gene has been observed in a number of organisms, including *Drosophila* (23), mouse (6, 33), and zebrafish (16). We have identified two alternatively spliced Dab1 isoforms in the chick retina, Dab1-E and Dab1-L, expressed at early and late stages of development, respectively (42). Dab1-L, normally referred to as Dab1, has the five tyrosine residues described earlier. Dab1-E is missing a 35-amino-acid (aa) region that includes Y198 and Y220, the major Reelin-induced Dab1 phosphorylation sites (43). Dab1-E also has

* Corresponding author. Mailing address: Department of Oncology, University of Alberta, Cross Cancer Institute, 11560 University Avenue, Edmonton, AB T6G 1Z2, Canada. Phone: (780) 432 8901. Fax: (780) 432 8892. E-mail: rgodbout@ualberta.ca.

† Supplemental material for this article may be found at <http://mc.manuscriptcentral.com/mcb>.

∇ Published ahead of print on 6 July 2010.

a 19-aa insertion located downstream of the tyrosine-rich domain (see Fig. 1). To address the role of Dab1-E in the retina, we have carried out a detailed analysis of Dab1-E expression during development. We demonstrate that Dab1-E is found primarily in retinal progenitor cells and that knockdown of Dab1-E affects the pool of progenitor cells in the retina. Our data suggest a tyrosine phosphorylation-independent and possibly Reelin-independent role for Dab1-E in the regulation of cell proliferation and commitment.

MATERIALS AND METHODS

Generation of anti-Dab1-E antibody. Rabbit anti-Dab1-E antiserum was generated by injecting rabbits with the KLH-conjugated Dab1-E peptide (LENGN LLLDIDEN, residues 207 to 220, specific to chicken Dab1-E) (SACRI Antibody Service, University of Calgary, Calgary, Canada). The antiserum was affinity-purified using a Dab1-E peptide-conjugated Affi-gel column (Bio-Rad).

Generation of pSUPER RNAi constructs. pSUPER RNA interference (RNAi) constructs were generated by ligating annealed oligonucleotides containing hairpin sequences targeting different regions of chicken *Dab1-E* mRNA into the pSUPER vector (Oligoengine) at the BglII and HindIII sites. Oligonucleotides were designated Dab1 *i*# (with “#” specifying the first nucleotide of the 19-nucleotide [nt] targeted region based on the Dab1-E cDNA sequence under GenBank accession no. AY242122). Five constructs targeting different regions of Dab1-E were tested: Dab1 i227, Dab1 i334, Dab1 i576, Dab1 i632, and Dab1 i1314. The Dab1 i632 oligonucleotide specifically targets Dab1-E, whereas the other four oligonucleotides target both the Dab1-E and Dab1-L isoforms.

Full-length Dab1-E and Dab1-L constructs with green fluorescent protein (GFP) fused at the N terminus have been previously described (42). To test the efficacy of the pSUPER Dab1 RNAi constructs, HEK293T or HeLa cells were cotransfected with pEGFP-Dab1-E and pSUPER Dab1 RNAi constructs by calcium phosphate-mediated DNA precipitation. GFP-Dab1-E levels in transiently transfected cells were compared by Western blot analysis using actin as a loading control.

Retroviral RNAi constructs. The avian retroviral RCASBP (B) vector system (21) was used to deliver small hairpin RNAs (shRNAs) into the eyes of developing chick embryos. Dab1 i576, identified as the most effective targeting oligonucleotide, and control scrambled oligonucleotide, under the control of the H1 promoter, were subcloned into the pSLAX12 Nco shuttle vector (37) at the EcoRI and HindIII sites. Next, the GFP coding region from the pEGFP-C1 vector was inserted into the pSLAX12 shuttle vector at the NcoI and SmaI sites upstream of the H1 promoter. After sequence verification, plasmids were digested with ClaI, releasing either the GFP-H1-Dab1 or scrambled oligonucleotide DNA fragment, which was then inserted into the ClaI site of RCASBP (B). This strategy results in GFP being placed under the control of the viral 5' long terminal repeat (LTR). All constructs were sequenced to ensure that no mutations were introduced during the cloning process.

In ovo electroporation of retroviral constructs. Fertilized eggs were obtained from a local supplier and incubated at 37°C for ~40 h prior to *in ovo* electroporation. At Hamburger Hamilton (HH) stages 10 to 12 (embryonic day 1.5 [ED1.5] to ED2) (26), eggs were windowed and 1.5 ml of albumin was removed. One to two μ l of RCASBP (B) DNA (3 μ g/ml) mixed with Fast Green was injected into the right optic vesicle of the embryo using a PV820 pneumatic picopump (World Precision Instruments, Inc.). Electrodes spaced 2 mm apart were placed so that the current passed through the right eye. Five square pulses of 15 V at 25 ms were applied using a BTX Electro Square Porator electroporator (ECM830). At ED5 or ED7, embryos were sacrificed and eyes were dissected and screened for GFP expression by epifluorescence. GFP-positive (GFP⁺) eyes were processed for further analysis.

Immunohistochemistry and immunofluorescence analysis. For immunohistochemistry, chick embryos or eyes were collected at specific developmental stages, fixed in formalin, and embedded in paraffin, as previously described (47). For immunofluorescence analysis, eyes were fixed in 4% paraformaldehyde, cryoprotected in a gradient of sucrose (12%, 16%, and 18%), and embedded in OCT. Antigen retrieval was done by microwaving in 0.01 M citrate (pH 6.0) for 20 min followed by blocking in 500 mM glycine. Antibodies used for immunohistochemistry were rabbit anti-Dab1-E (1:400), rabbit anti-Dab1 B3, a gift from Jonathan Cooper, Fred Hutchinson Cancer Research Center (1:500), rabbit anti-ApoER2 2562, a gift from Joachim Herz, University of Texas Southwestern Medical Center (1:2,000), and mouse anti-Reelin (553730; Calbiochem) (1:1,000). Antibodies used for immunofluorescence analysis were rabbit anti-Dab1-E (1:400),

mouse anti-BrdU (1170376; Roche) (1:100), mouse anti-Islet-1 (39.4D5; 1:1,500; University of Iowa Hybridoma Bank), mouse anti-AP2 α (3B5; University of Iowa Hybridoma Bank) (1:250), goat anti-GFP (ab6673; Abcam) (1:2,000), mouse anti-TUJ1 (MMS-435P; Covance) (1:2,000), mouse anti-proliferating cell nuclear antigen (anti-PCNA) (N1529, Dako) (1:5,000), mouse anti-glutamine synthetase (610517; BD Bioscience) (1:500), rabbit anti-phospho-histone H3 serine 10 (ab5176; Abcam) (1:5,000), and sheep anti-Chx10 antibody (a gift from Rod Bremner, University of Toronto, Toronto, Canada; 1:3,000). The Dab1-E peptide competition assay was carried out by adding Dab1-E peptide to the diluted anti-Dab1-E antibody at a concentration of 0.1 μ M.

Quantitative analyses of BrdU, CHX10, and phospho-histone H3. For BrdU labeling, 1 to 2 μ l of a 1 mM BrdU solution was injected into the right eye of chick embryos 3 h prior to collection at ED5. To verify reduction in Dab1-E levels in GFP⁺ cells and measure the percentage of BrdU⁺ cells in regions of the retina with reduced levels of Dab1-E, we immunostained two consecutive tissue sections with either goat anti-GFP (1:2,000) and rabbit anti-Dab1-E (1:400) antibodies or goat anti-GFP and mouse anti-BrdU (1:100) antibodies. Micrographs were collected using a Zeiss Axio Imager Z1 microscope with a 40 \times lens.

BrdU⁺ and GFP⁺ cells were counted using the Metamorph software program. The percentage of BrdU⁺ cells was obtained by dividing the number of BrdU⁺ cells by the total number of GFP⁺ cells or Hoechst 33342-stained cells in peripheral, intermediate, and central areas of the retina. This analysis was carried out on 6 eyes obtained from control embryos, 6 eyes obtained from embryos electroporated with the scrambled shRNA construct, and 8 eyes electroporated with the Dab1 shRNA construct. Data were analyzed using Metamorph and exported to the Excel software program. Statistical analysis was performed with one-way analysis of variance (ANOVA) or Student's *t* test.

CHX10⁺ and GFP⁺ cells were counted using Metamorph software as described above. Analysis was carried out at ED5 on 4 eyes electroporated with the scrambled shRNA construct and 4 eyes electroporated with the Dab1 shRNA construct.

Quantification of phospho-histone H3⁺ and GFP⁺ cells in ED5 retinal sections was carried out on 6 eyes electroporated with the scrambled shRNA construct and 8 eyes electroporated with the Dab1 shRNA construct.

Western blot analysis and immunoprecipitations. Chick retina, stomach, liver, brain, heart, gut, and retinal cultures were lysed in radioimmunoprecipitation assay (RIPA) buffer (50 mM Tris-HCl pH 7.5, 150 mM NaCl, 1% Triton X-100, 0.5% sodium deoxycholate, 0.1% SDS, 50 mM NaF, 1 mM phenylmethylsulfonyl fluoride [PMSF], 1 mM Na₃VO₄, and 1 \times complete protease inhibitor cocktail [Roche]). To maximize the separation between the different Dab1-E isoforms, cell lysates were electrophoresed through a 20-cm by 20-cm 8% polyacrylamide-SDS gel for 5 h. The following antibodies were used for Western blot analysis: rabbit anti-Dab1-E (1:500), rabbit anti-Dab1 (100-4101-225; 1:5,000; Rockland), goat anti-Dab1 (AB9012; 1:500; Chemicon), rabbit anti-Dab1 (B3; 1:1,000), mouse antiactin (A5441; 1:100,000; Sigma), goat anti-GFP (ab6673; 1:2,000; Abcam), rabbit anti-ApoER2 2562 (1:2,000), mouse anti-CrkL (05-414; 1:2,000; Millipore), and mouse anti-Reelin (553730; 1:500; Calbiochem).

For immunoprecipitation, cell lysates were precleared with protein A or protein G Sepharose beads (GE Healthcare) for 1 h at 4°C, followed by incubation with primary antibodies or IgG control overnight at 4°C and collection of the immunoprecipitates with protein A or protein G Sepharose beads. Immunoprecipitates or cell lysates were separated by SDS-PAGE, blotted onto nitrocellulose membranes, and immunostained with the appropriate antibodies.

Dissociation of chick retinal cells and immunofluorescence analysis. Retinas from scrambled or Dab1 shRNA-electroporated embryos at ED7 were screened for GFP expression by epifluorescence. For comparison, only GFP⁺ retinal tissues from similar locations were used for analysis. GFP⁺ retinal tissues were dissociated with trypsin and collagenase as previously described (1). Cells were plated on 100 μ g/ml poly-D-lysine-coated glass coverslips and incubated at 37°C for 2 h before immunofluorescence analysis.

For immunofluorescence analysis, cells were fixed in 4% paraformaldehyde for 10 min, permeabilized in 0.1% Triton X-100 for 5 min, and blocked in 1% normal donkey serum for 1 h. Cells were then incubated with primary antibodies (1:4,000 goat anti-GFP, 1:1,500 mouse anti-Islet-1, and 1:500 mouse anti-AP2 α) overnight at 4°C, followed by incubation with Alexa dye-conjugated secondary antibodies for 2 h. For quantification of Islet-1⁺ and AP2 α ⁺ cells in retinal tissue electroporated with RCAS constructs, we collected micrographs in the tile scan (mosaic scan) mode (3 \times 3) using a confocal microscope (LSM 710) and a 20 \times lens. The number of immunoreactive cells was scored using Metamorph software. A minimum of three independently electroporated retinas were analyzed, with three tile scan images from each retina.

Primary retinal cultures and Reelin treatment. Primary retinal cultures were prepared by trypsinizing ED5 to ED5.5 or ED10 retinas and plating the disso-

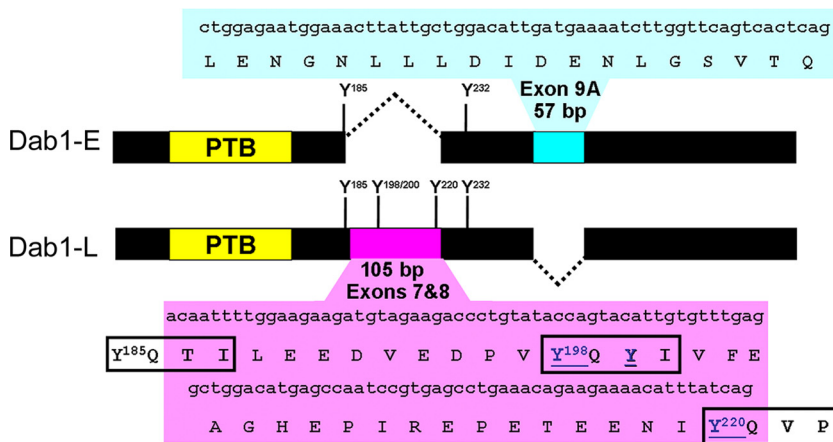


FIG. 1. Schematic diagram of exon exclusion and inclusion in Dab1 isoforms. The two exons deleted in Dab1-E but included in Dab1-L are shown in magenta; the exon included in Dab1-E but excluded from Dab1-L is shown in blue. The phosphotyrosine binding (PTB) domain common to both Dab1 isoforms is shown in yellow. Two tyrosines, at 185 and 232, are indicated in Dab1-E. Five tyrosines, at 185, 198, 200, 220, and 232, are indicated in Dab1-L. Alternative splicing converts Y¹⁸⁵QTI (in Dab1-L) to Y¹⁸⁵QVP (in Dab1-E). YQXI is a consensus Src family kinase phosphorylation site, whereas YXVP is a consensus Abl family kinase recognition site.

ciated cells in Dulbecco's modified Eagle medium supplemented with 10% fetal calf serum and penicillin-streptomycin. For generation of Reelin-conditioned medium, HEK293T cells at 50% confluence were transfected with pCrl-Reelin (a gift from Tom Curran, University of Pennsylvania) or pcDNA3 constructs. The medium was replaced with Opti-MEM 1 (Invitrogen) 24 h after transfection. Supernatants were collected 36 h later and concentrated 30× using Amicon Ultra centrifugal filter devices (100,000 molecular-weight cutoff [MWCO]; Millipore). ED10 primary retinal cells were treated for 15 min with concentrated supernatants diluted 1:15.

Drug treatment and reverse transcription (RT)-PCR analysis. ED5.5 primary retinal cultures were treated with dimethyl sulfoxide (DMSO), 20 μM cyclopamine (Calbiochem), and 10 μM DAPT (Calbiochem) for 24 h, followed by total RNA extraction using the TRIzol reagent (Invitrogen). Five μg total RNA from ED5.5 primary retinal cells treated with DMSO, cyclopamine, and DAPT were reverse transcribed using an oligo(dT) primer and Superscript reverse transcriptase (Invitrogen). Single-strand cDNAs were PCR amplified using the primers P1, P2, P3, and P4 (42). PCR products were run on a 9% polyacrylamide gel.

RESULTS

Expression of Dab1-E and Dab1-L in the developing chick retina. We have identified two main isoforms of Dab1 in chick retina and brain: Dab1-E, previously shown by RT-PCR and *in situ* hybridization analysis to be expressed at early stages of retinal development, and Dab1-L, found primarily in ganglion and amacrine cells (42). To carry out a more detailed analysis of the spatial and temporal Dab1-E distribution pattern, we generated anti-Dab1-E antiserum by immunizing rabbits with a Dab1-E-specific peptide (encoded by exon 9A, shown in Fig. 1). The specificity of the anti-Dab1-E antiserum was determined by Western blot analysis of chick retinal cells transfected with a GFP, GFP-Dab1-E, or GFP-Dab1-L expression construct. As shown in Fig. 2A, a commercially available anti-Dab1 antibody raised against the C terminus of Dab1 recognized both the GFP-Dab1-E and GFP-Dab1-L proteins and at least five lower-molecular-weight bands. The anti-Dab1-E antiserum specifically recognized GFP-Dab1-E, as well as lower-molecular-weight bands which were also observed in untransfected cells.

Next, we examined endogenous Dab1-E and Dab1-L expres-

sion in chick retinal tissues at different stages of development. At ED5, when 85% of retinal cells are proliferating (19), similar banding patterns (consisting of at least 4 bands) were observed using either the anti-Dab1 antibody or the anti-Dab1-E antiserum (Fig. 2B). At ED7, when 60% of cells are proliferating, immunostaining with either anti-Dab1-E or anti-Dab1 antibody revealed the same four bands detected at ED5. However, a weakly staining, slower-migrating band (indicated by the asterisk) was also detected with anti-Dab1 antibody. This slower-migrating band was prominently displayed at later developmental stages (ED10, ED15, and posthatching day 1 [P1]) using anti-Dab1 but not anti-Dab-E antibodies. The four lower bands recognized by both the anti-Dab1 and anti-Dab1-E antibodies remained abundant at ED10 but were greatly reduced in intensity by ED15 and barely detectable in the fully differentiated P1 retina (Fig. 2B). Our data indicate that the slower-migrating band represents Dab1-L while the four faster-migrating bands likely represent different forms of Dab1-E.

Since bands extraneous to Dab1/Dab1-E were observed upon immunostaining with anti-Dab1-E serum, we affinity purified this serum using a Dab1-E peptide-conjugated Affi-gel column. Immunoblot analysis of ED5 retina using the affinity-purified anti-Dab1-E antibody produced results identical to that obtained with anti-Dab1 antibody, demonstrating the specificity of the anti-Dab1-E antibody (Fig. 2C). Using the anti-Dab1-E antibody, we carried out Western blot analysis of brain lysates at different stages of development (ED3 to ED10). Dab1-E was expressed in brain at all developmental stages examined, albeit at lower levels than in the retina (Fig. 2C). In contrast, Dab1-L was first detected in the brain at ED7. Other tissues, such as liver, stomach, and gut, also expressed Dab1-E. The slower-migrating Dab1-L was not detected in these tissues (Fig. 2D), suggesting tissue-specific alternative splicing of Dab1 pre-mRNA during development. Of note, Dab1-E was barely detectable in ED5 heart; however, we observed a strong band migrating at ~66 kDa in ED9 heart upon

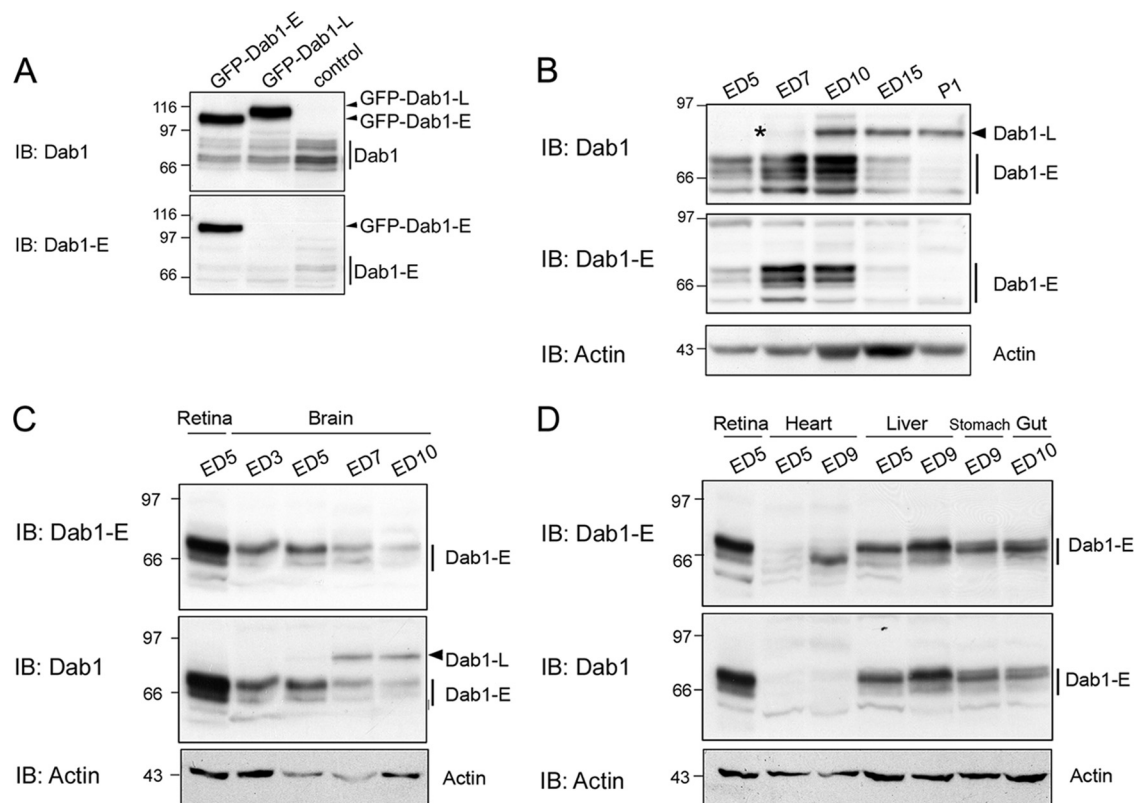


FIG. 2. Dab1 expression in the chicken embryo. (A) Determination of anti-Dab1-E antibody specificity. Fifty μ g cell lysates prepared from ED5 retinal cultures transfected with GFP (control), GFP-Dab1-E, or GFP-Dab1-L expression constructs were resolved by 8% SDS-PAGE and transferred to a polyvinylidene difluoride (PVDF) membrane. The membrane was immunostained with anti-Dab1 (raised against the C terminus of Dab1, top panel) or anti-Dab1-E (raised against the E-specific region, bottom panel) antibody. Anti-Dab1 antibody recognizes both Dab1-E and -L, whereas the anti-Dab1-E antibody specifically recognizes Dab1-E. The endogenous Dab1 and Dab1-E proteins are indicated by vertical bars. IB, immunoblot. (B) Western blot analysis of Dab1 in the chick retina. To maximize the separation between the Dab1 isoforms, 100 μ g retinal cell lysates prepared from ED5, ED7, ED10, ED15, and P1 were resolved on a 20-cm by 20-cm 8% SDS acrylamide gel and transferred to a PVDF membrane. The membrane was immunostained with anti-Dab1 (top panel) or anti-Dab1-E (middle panel) antibody. The arrowhead indicates Dab1-L, whereas the vertical bars show the early form(s) of Dab1 (Dab1-E). The asterisk indicates a weakly stained Dab1-L band in ED7 retina. (C) Western blot analysis of Dab1 in the chick brain. Cell lysates prepared from ED5 chick retina, ED3 chick head, ED5, ED7, and ED10 chick brain were analyzed by Western blotting as indicated in panel A. (D) Western blot analysis of Dab1 in embryonic chick tissues. Cell lysates prepared from chick retina, heart, stomach, liver, and gut at different developmental stages (as indicated) were analyzed by Western blotting. Actin was used as a loading control.

staining the blot with anti-Dab1-E but not anti-Dab1 antibody. Since the anti-Dab1 antibody was generated against the C terminus of Dab1, this suggests that heart tissue expresses a third isoform of Dab1 that contains the Dab1-E-specific region but lacks the C terminus of Dab1.

Distribution of Dab1-E and Dab1-L in the developing chick retina. To examine the cellular distribution of Dab1-E and Dab1-L in the developing retina, we carried out immunohistochemical analysis of serial retinal sections. For these analyses, we used anti-Dab1 B3 antibody raised against the central domain of mouse Dab1 (aa 107 to 243), including the tyrosine phosphorylation domain (33). When this antibody was used for Western blot analysis of ED10 chick retina lysates, it was found to specifically recognize the slower-migrating band, Dab1-L (see Fig. S1 in the supplemental material). This suggests that the epitopes recognized by the anti-Dab1 B3 antibody are located within the tyrosine-rich region that is excluded in Dab1-E.

We used anti-Dab1 B3 and anti-Dab1-E antibodies to

specifically examine the temporal and spatial distribution of Dab1-L and Dab1-E in the developing retina. At ED4, when the vast majority of retinal cells are proliferating (>90%), cytoplasmic Dab1-E was found throughout the retina with slightly stronger staining in the emerging ganglion cell layer (GCL). The B3 antibody produced a weak background signal with slightly stronger staining of the emerging ganglion cells (Fig. 3A). At ED5, the B3 antibody generated a strong signal in the GCL whereas Dab1-E staining intensity was similar throughout the retina (Fig. 3B). At ED7, Dab1-E was abundantly expressed throughout the retina with the exception of the GCL. Dab1-L remained prominent in ganglion cells. At ED8 and ED9, during the peak of amacrine and photoreceptor cell accumulation (50), we observed elevated levels of Dab1-E in the inner nuclear layer (INL), with reduced staining in the outer nuclear layer (ONL) where photoreceptors are located (Fig. 3D and E). Dab1-L was prominently expressed in amacrine cells at ED8 and ED9.

By ED11 (toward the end of retinal neurogenesis), Dab1-E

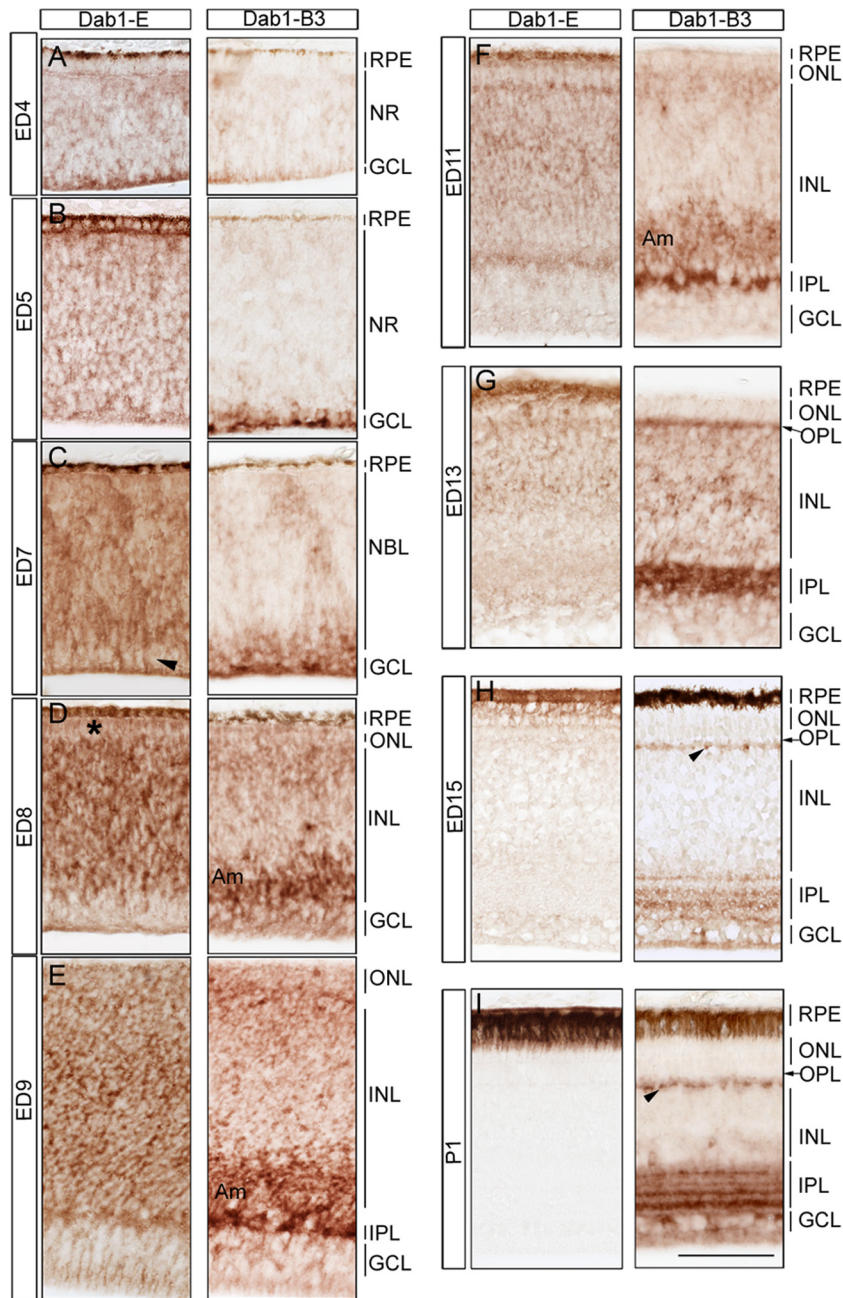


FIG. 3. Immunohistochemical analysis of Dab1 isoforms in the developing chick retina. Consecutive sections from formalin-fixed paraffin-embedded chick retina at different developmental stages (as indicated) were immunostained with anti-Dab1-E or anti-Dab1 B3 antibody. Sections were not counterstained in order to better visualize Dab1 staining. The arrowhead in panel C points to the reduced expression of Dab1-E in the GCL. In panel D, the asterisk indicates the reduced levels of Dab1-E in the emerging ONL. Abbreviations: RPE, retinal pigmented epithelium; NR, neural retina; NBL, neuroblastic layer; INL, inner nuclear layer; IPL, inner plexiform layer; GCL, ganglion cell layer; ONL, outer nuclear layer; OPL, outer plexiform layer; Am, amacrine. Scale bar, 50 μ m.

levels were significantly reduced in the retina, with residual staining in the middle of the INL (Fig. 3F). Dab1-L was abundantly expressed in the inner plexiform layer (IPL) and in amacrine cells. At ED13, Dab1-L was strongly expressed in the IPL and to a lesser extent in the outer plexiform layer (OPL). Two days later, Dab1-E was barely detectable in the retina whereas Dab1-L was found in the IPL and OPL, with a distinct layering pattern in the IPL, in keeping with the reported

expression of Dab1 (Dab1-L) in distinct subsets of amacrine and ganglion cells (52). Shortly after hatching at P1, intense Dab1-L staining was observed in the IPL, ganglion fibers, and in a layer of cells located in the outer part of the INL (likely horizontal cells based on location, indicated by the arrowheads in Fig. 3H and I).

Competition experiments with the Dab1-E peptide confirmed that the signal detected with the Dab1-E antibody was

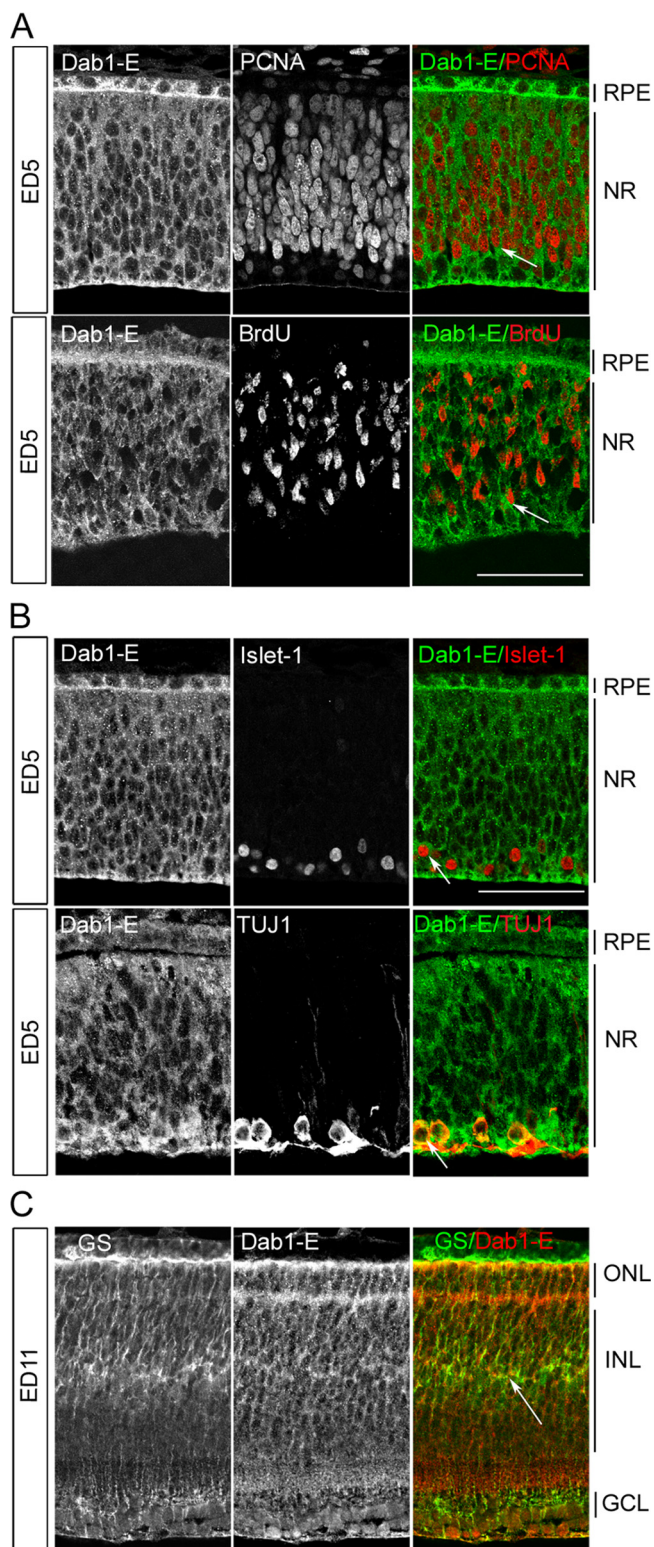


FIG. 4. Expression of Dab1-E in proliferating retinal progenitor cells and newly committed postmitotic cells. (A) Coimmunostaining of Dab1-E and PCNA or Dab1-E and BrdU in ED5 chick retina. Retinal sections were doubly stained with rabbit anti-Dab1-E (1:400) and either mouse anti-PCNA (1:5,000) or mouse anti-BrdU (1:50) antibodies, followed by donkey anti-rabbit and donkey anti-mouse secondary antibodies conjugated with fluorescent Alexa 488 and Alexa 555, respectively. Arrows indicate the colabeling of Dab1-E (cytoplasmic) and

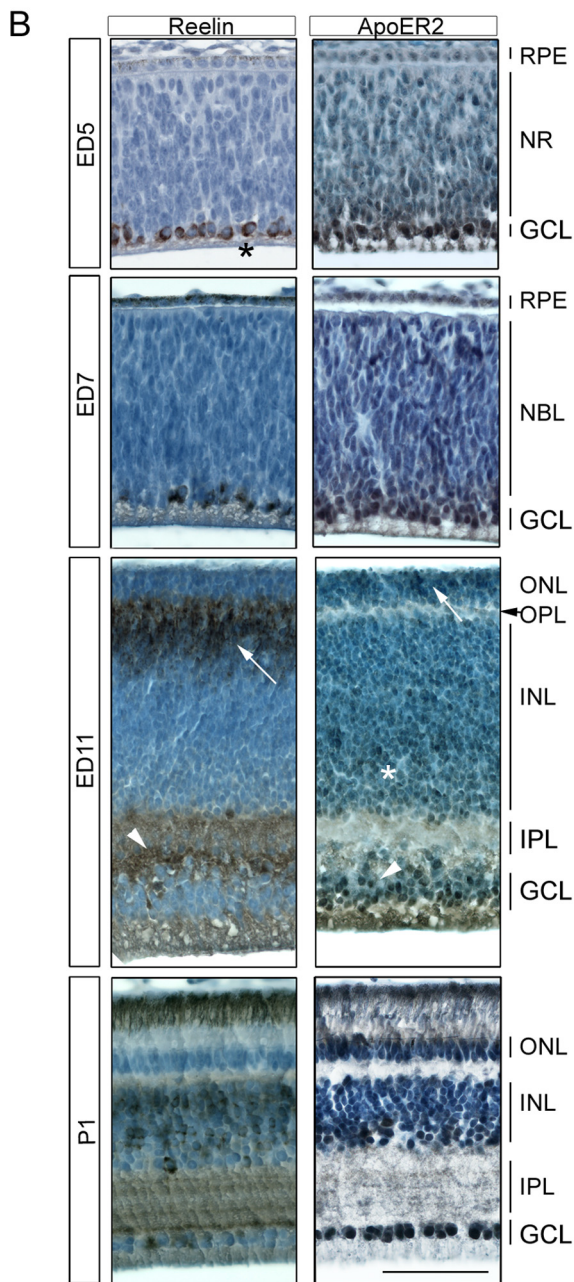
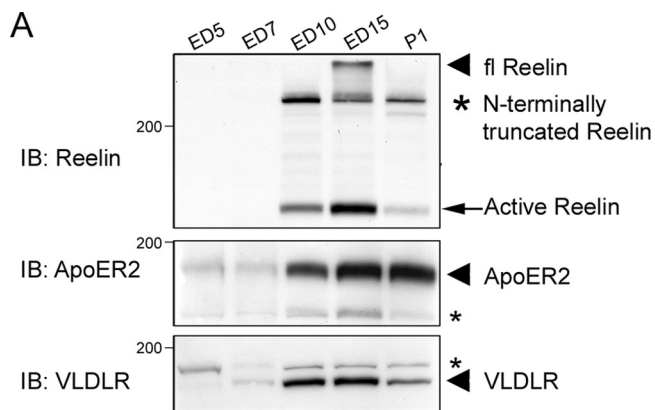
specific to Dab1-E (see Fig. S2 in the supplemental material). Immunostaining with an anti-Dab1 antibody (raised against the N terminus of Dab1) that recognizes both Dab1-E and Dab1-L revealed a Dab1-E/Dab1-L-specific expression pattern at ED5, a mixed Dab1-E/Dab1-L expression pattern at ED7 and ED11, and a Dab1-L-specific expression pattern at P1 (see Fig. S2 in the supplemental material). Together our data demonstrate that Dab1-E and Dab1-L have distinct temporal and spatial distribution patterns in the developing retina, with Dab1-E being expressed primarily in neuroblastic cells and newly committed cells and Dab1-L being first expressed in ganglion, followed by expression in amacrine and horizontal cells at later developmental stages. Particularly striking is the intensity of the Dab1-L signal in the IPL from ED9 to posthatching.

Expression of Dab1-E in proliferating cells and in newly committed postmitotic cells. The spatial and temporal distribution pattern of Dab1-E suggests a role specific to progenitor cells during retinal development. To directly address whether Dab1-E is expressed in actively proliferating cells, we coimmunostained ED5 retinal tissue with antibodies to Dab1-E and the proliferation marker PCNA. As shown in Fig. 4A, Dab1-E and PCNA localize to the same cells throughout most of the retina. Ganglion cells are positive for Dab1-E but negative for PCNA. By injecting BrdU into the eyes of ED5 chick embryos, we showed that Dab1-E colocalizes with BrdU⁺ cells (Fig. 4A). Our combined data indicate that Dab1-E is found predominantly in proliferating retinal progenitor cells at early stages of development.

In addition to proliferating cells, Dab1-E is transiently expressed in postmitotic retinal cells. For example, Dab1-E is detected in ganglion cells at ED5 but is excluded from ganglion cells by ED8 (Fig. 3B and E). Similarly, Dab1-E is expressed in amacrine cells at ED8 but is excluded from these cells by ED13 (Fig. 3D and G). Furthermore, the distribution pattern of Dab1-E at ED11 suggests that Dab1-E may also be found in Müller glial cells, last to differentiate in chick retina (Fig. 3F; see also Fig. S2C in the supplemental material).

To verify that Dab1-E is indeed expressed in ganglion cells at ED5, we carried out coimmunofluorescence analysis of Dab1-E and either Islet-1, a marker of retinal ganglion cells (4), or class III β -tubulin TUJ1, a marker of postmitotic neurons. As shown in Fig. 4B, Dab1-E and Islet-1 are coexpressed in retinal ganglion cells at ED5. We also observed costaining of TUJ1 and Dab1-E in ganglion cells (Fig. 4B). To determine whether Dab1-E is transiently expressed in Müller glial cells,

PCNA (nuclear) or BrdU (nuclear) in retinal cells. (B) Coimmunostaining of Dab1-E and Islet-1 or Dab1-E and TUJ1 in ED5 chick retina. Retinal sections were doubly stained with rabbit anti-Dab1-E and mouse anti-Islet-1 (1:1,500) or mouse anti-TUJ1 (1:2,000) antibodies as indicated in panel A. Arrows indicate the colabeling of Dab1-E and Islet-1 or TUJ1 in retinal cells. (C) Coimmunostaining analysis of Dab1-E and glutamine synthetase (GS) in ED11 chick retina. Retinal sections were doubly stained with rabbit anti-Dab1-E and mouse anti-GS (1:500) antibodies, followed by donkey anti-rabbit or donkey anti-mouse secondary antibodies conjugated with Alexa 555 and Alexa 488, respectively. Arrows indicate the colabeling of Dab1-E and GS in ED11 chick retina. Micrographs were collected with a Zeiss LSM 510 confocal microscope equipped with a 40 \times lens. For abbreviations, see the legend for Fig. 3. Scale bar, 50 μ m.



we carried out coimmunofluorescence analysis of Dab1-E with glutamine synthetase (GS), a marker of Müller glial cells. At ED11, the peak of Müller glia cell generation (50), we observed costaining of Dab1-E and GS in the middle of the INL (Fig. 4C), indicating that Dab1-E is expressed in Müller glial cells. At P1, Dab1-E could no longer be detected in Müller glial cells (Fig. 3I), demonstrating the transitory nature of Dab1-E expression in these cells.

Expression of Reelin and its receptors in the developing chick retina. Previous studies have demonstrated that Dab1 (i.e., Dab1-L) functions through Reelin and its receptors VLDLR and ApoER2 (35, 58). Although Dab1-E retains the PI/PTB domain, required for interaction with Reelin receptors, it is not clear whether Dab1-E activity in the developing retina requires Reelin and its receptors. To examine the temporal expression of Dab1-E in relation to Reelin and its receptors, we carried out Western blot analysis with the same retinal cell lysates used to generate Fig. 2B. Reelin was not detected at ED5; however, weak bands were visible at ED7 upon longer exposure (Fig. 5A and data not shown). Three bands, representing full-length Reelin (top band), N-terminally truncated Reelin (middle band), and the active form of Reelin (bottom band) (44), were observed at ED10, with peak levels of active Reelin at ED15. Immunohistochemical analysis revealed prominent Reelin expression in ganglion cells at both ED5 and ED7 (Fig. 5B). By ED11, high levels of Reelin were observed in bipolar cells (arrow), some of the cells in the GCL (arrowhead), OPL, and IPL. At P1, Reelin was primarily found in bipolar cells and in the plexiform and fiber layers. These results are consistent with the Reelin mRNA and protein expression patterns previously reported for chick and mouse retina (9, 54).

Both ApoER2 and VLDLR were detected in the ED5 and ED7 retina by Western blot analysis (Fig. 5A); however, protein levels were lower than those observed at ED10 and ED15. Two forms of ApoER2 and VLDLR were observed in the retina, consistent with previous reports indicating that these

FIG. 5. Expression of Reelin, ApoER2, and VLDLR in the developing chick retina. (A) Western blot analysis of Reelin, ApoER2, and VLDLR in the developing chick retina. Western blotting of Reelin, ApoER2, and VLDLR was carried out as described in the legend for Fig. 2B. The membrane was immunostained with anti-Reelin (1:500, top panel), ApoER2 (1:2,000, middle panel), or VLDLR (1:200, bottom panel) antibodies, respectively. Actin was used as a loading control. The arrowhead in the top panel indicates full-length Reelin, whereas the large asterisk and the arrow indicate N-terminally truncated Reelin and active Reelin, respectively. Arrowheads in the middle and bottom panels indicate the most abundant forms of ApoER2 and VLDLR, whereas small asterisks indicate alternatively spliced isoforms. (B) Immunohistochemical analysis of Reelin and ApoER2 in the developing chick retina. Chick retinal sections at different developmental stages (as indicated) were immunostained with mouse anti-Reelin (1:500) or rabbit anti-ApoER2 (1:2,000) antibodies, and nuclei were labeled with hematoxylin. At ED5, the asterisk (left panel) indicates Reelin expression in ganglion cells. At ED11, the arrow and arrowhead (left panel) point to the expression of Reelin in bipolar and ganglion cells, respectively. The arrow, asterisk, and arrowhead (right panel) indicate ApoER2 expression in a subset of photoreceptors and amacrine and ganglion cells in ED11 chick retina. For abbreviations, see the legend for Fig. 3. Scale bar, 50 μ m.

two receptors have alternatively spliced isoforms (38, 57). Immunohistochemical analysis of ApoER2 revealed intense staining of ganglion cells at ED5 and ED7 (Fig. 5B). ApoER2 expression was widespread at ED11, whereas the ApoER2 signal was strongest in ganglion cells, amacrine cells, and a subset of photoreceptor cells at P1. These data indicate that there is a good correlation between the expression patterns of Reelin, ApoER2, VLDLR, and Dab1-L in the developing retina, in keeping with a role for Dab1-L in Reelin-mediated signaling. However, there is little correlation between the expression pattern of Dab1-E and that of Reelin and its receptors, suggesting that Dab1-E may function independently of Reelin signaling.

Dab1-E is not tyrosine phosphorylated and does not interact with CrkL in the developing retina. A major difference between Dab1-E and Dab1-L is the absence of two tyrosine phosphorylation sites (Y198 and Y220) implicated in the relay of the Reelin signal in Dab1-E. As the Y185 phosphorylation site is converted from a Src to an Abl recognition site (Y¹⁸⁵QTI → Y¹⁸⁵QVP) in Dab1-E (42), a consequence of Dab1 alternative splicing is the loss of two consensus SFK phosphorylation sites and the retention of two consensus Abl phosphorylation sites in Dab1-E (Fig. 1). In previous reports, we have shown that exogenous GFP-Dab1-L but not GFP-Dab1-E is robustly tyrosine phosphorylated in transfected retinal cells (41–42).

As indicated earlier, 4 bands are detected in retinal lysates immunostained with anti-Dab1-E antibody (Fig. 2B), suggesting Dab1-E posttranslational modification. To investigate whether endogenous Dab1-E is tyrosine phosphorylated, we immunoprecipitated Dab1 from ED10 retinal lysates using an anti-Dab1 antibody that recognizes both Dab1-E and Dab1-L. We selected ED10 for our analyses because of the relative abundance of both Dab1-E and Dab1-L at this developmental stage. Immunoprecipitates were immunoblotted with an antiphosphotyrosine antibody (clone 4G10; Millipore). As shown in Fig. 6A, the antiphosphotyrosine antibody recognized Dab1-L but none of the Dab1-E bands. Dab1-L identity was confirmed by reprobing the blot with anti-Dab1 antibody, which also revealed the presence of the non-tyrosine-phosphorylated Dab1-E bands. We used two additional phosphotyrosine antibodies (pY 1000 and pY PT-66) to verify that Dab1-E was not tyrosine phosphorylated (data not shown).

Next, we addressed the possibility that Reelin stimulation might induce Dab1-E tyrosine phosphorylation. ED10 primary retinal cultures (which also express endogenous Reelin) were treated with Reelin-conditioned medium. As shown in Fig. 6B, Reelin treatment induced Dab1-L tyrosine phosphorylation by ~2× in retinal cultures but had no effect on Dab1-E. These data indicate that Dab1-E is not tyrosine phosphorylated in response to exogenous Reelin treatment, and they are consistent with a Reelin-independent role for Dab1-E.

Reelin signaling promotes association of Dab1 with Crk adaptors, CrkII and CrkL (15). *CrkII*^{-/-} *CrkL*^{-/-} double knockout mice exhibit phenotypes similar to that of *reeler* mice but retain normal Reelin-induced Dab1 tyrosine phosphorylation. However, two downstream Reelin-Dab1-dependent signaling events, phosphorylation of guanine nucleotide exchange factor C3G and Akt phosphorylation, are abolished in the double knockout mice, suggesting that Crk proteins play

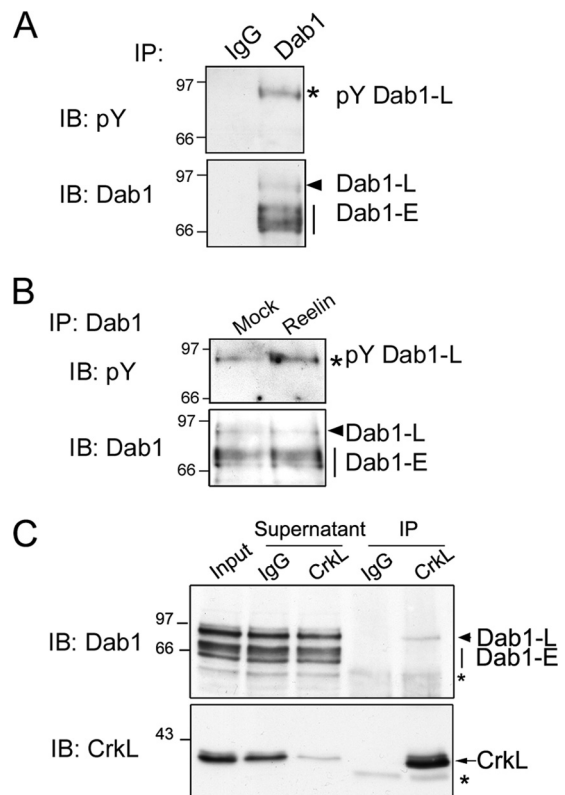


FIG. 6. Examination of Dab1 tyrosine phosphorylation in the retina. (A) Tyrosine phosphorylation of Dab1-L in ED10 chick retina. Western blotting of anti-Dab1 antibody and IgG control immunoprecipitates from ED10 chick retinal extracts was carried out as for Fig. 2A. The membrane was immunostained with mouse anti-pY 4G10 and rabbit anti-Dab1 antibodies. (B) Reelin stimulates Dab1-L tyrosine phosphorylation but not that of Dab1-E in ED10 retinal cells. ED10 primary retinal cultures were treated with mock or Reelin-conditioned medium for 15 min, followed by cell lysis in RIPA buffer. Dab1 proteins were immunoprecipitated from the cell lysates and analyzed by Western blotting. Tyrosine-phosphorylated Dab1 was detected with a mouse anti-pY 4G10 antibody, and Dab1 identity was confirmed with an anti-Dab1 antibody. (C) Dab1-L but not Dab1-E associates with CrkL. Immunocomplexes were immunoprecipitated from ED10 chick retinal lysates by use of mouse anti-CrkL or mouse IgG control. The immunoprecipitates, supernatants, and 10% input were analyzed by Western blotting using anti-Dab1 and CrkL antibodies. Asterisks indicate nonspecific bands.

essential roles downstream of Dab1 (49). Two YXVP sites (Y220 and Y232) in Dab1 have been shown to be critical for the recruitment of Crk proteins (5). Like Dab1-L, Dab1-E contains two YXVP sites (converted Y185 and Y232). To determine whether both Dab1-L and Dab1-E can interact with CrkL, we carried out coimmunoprecipitation experiments with proteins extracted from ED10 retina, when both Dab1-E and Dab1-L are relatively abundant. As shown in Fig. 6C, only Dab1-L coimmunoprecipitates with CrkL proteins, suggesting that tyrosine phosphorylation is required for interaction with CrkL and that only Dab1-L can transmit the signal to CrkL and downstream molecules.

Knockdown of Dab1-E in the developing retina. Dab1-E expression in proliferating retinal progenitor cells and postmitotic cells suggests that Dab1-E may be important in

retinal cell proliferation and/or commitment. To examine the role of Dab1-E in the retina, we used RNAi to knockdown Dab1-E at early stages of retinal development. Five RNAi constructs were tested (including one that specifically targets Dab1-E, Dab1 i632). Of these five RNAi constructs, Dab1 i576 was the most effective at reducing Dab1-E levels in HeLa and HEK293T cells cotransfected with the GFP-Dab1-E expression construct (see Fig. S3A in the supplemental material) (data not shown). A significant decrease in the GFP-Dab1-E level was also observed in cells cotransfected with Dab1 i334.

To test whether these two shRNAs (Dab1 i576 and Dab1 i334) are also effective at reducing Dab1-E levels in chick retinal cells, we cotransfected ED5 primary retinal cultures with the GFP-Dab1-E expression construct along with the pSUPER Dab1 RNAi constructs. Both RNAi constructs suppressed exogenous GFP-Dab1-E expression in chick retinal cells (see Fig. S3B in the supplemental material).

To maximize our transfection/infection efficiency, we subcloned GFP-H1-Dab1 i576 or GFP-H1-scrambled cassettes from pSUPER-RNAi constructs into the replication-competent avian retroviral vector RCAS. GFP, under the control of the 5' LTR, allows identification of cells infected with the RCAS constructs (as illustrated in Fig. S3C in the supplemental material). This RCAS-GFP-Dab1 i576 construct effectively reduced the levels of exogenous GFP-Dab1-E (see Fig. S3D) and endogenous Dab1-E and Dab1-L (see Fig. S3E and S3F) in primary retinal cultures.

GFP-Dab1 i576 or GFP-scrambled constructs were introduced into chick embryos at stages 10 to 12 (ED1.5 to ED2) by *in ovo* electroporation. Since Dab1 i576 targets a region shared by both Dab1-E and Dab1-L, we terminated the experiments at either ED5 or ED7 (when Dab1-L levels are very low) to specifically address the role of Dab1-E in early retinal development. Immunostaining analysis revealed significantly reduced Dab1-E expression in the GFP⁺ regions of both ED5 (Fig. 7A) and ED7 (Fig. 7B) retinas electroporated with RCAS Dab1 i576. In general, the reduction in Dab1-E expression was most apparent in the vitreal (inner) part of the retina. Scrambled shRNAs had no effect on Dab1-E staining.

Knockdown of Dab1-E in the developing retina reduces cell proliferation and affects nuclear distribution of progenitor cells. Since disruption of the Reelin-Dab1 signaling pathway causes extensive migration and lamination defects in the developing brain (17, 34), we first examined the gross architecture of the retina with reduced Dab1-E levels. The overall structure of the retina appeared normal at both ED5 and ED7, with no apparent laminar defects associated with Dab1-E knockdown (data not shown).

The expression pattern of Dab1-E in proliferating cells and newly committed cells is compatible with a role in neurogenesis. We therefore examined the effect of Dab1-E knockdown on retinal cell proliferation. BrdU was injected into the eyes of ED5 chick embryos (approximately 68 h after *in ovo* electroporation) in order to label S-phase cells. Eyes were harvested 3 h after BrdU injection and processed for immunostaining. Since there is a strong central-to-peripheral differentiation gradient in the developing retina, we first measured BrdU incorporation in the peripheral, intermediate, and central zones of six nonmanipulated normal ED5 retinas (see Fig. S4 in the supplemental material). Two micrographs from each of the

three zones were collected, and cells positive for BrdU and Hoechst 33342 were scored using Metamorph software. The percentage of BrdU⁺ cells in the total cell population was 45 to 50% regardless of the zone examined, consistent with previous reports demonstrating that the central-to-peripheral differentiation gradient (as measured by cell proliferation) is not apparent until ED6 in the chick retina (50).

We then carried out BrdU labeling experiments with electroporated embryos at ED5. To exclude the possibility that *in ovo* electroporation might affect cell proliferation, we first compared the BrdU labeling index (percentage of BrdU⁺ cells in GFP⁺ cells) in scrambled shRNA-electroporated retinas versus control retinas. Although the BrdU labeling index was slightly decreased for the scrambled shRNA-electroporated retinas over that for the control, the difference was not statistically significant (Fig. 8). Next, we compared the BrdU labeling index for retinas electroporated with scrambled versus Dab1 shRNA. The BrdU labeling index was significantly reduced in the Dab1-E knockdown group (25% [$n = 8$] versus 42% [$n = 6$]; $P < 0.01$) (Fig. 8), suggesting a role for Dab1-E in cell proliferation.

CHX10 is expressed in retinal progenitor cells at early stages of retinal development (8). To determine whether the number of progenitor cells was decreased upon Dab1-E knockdown, we compared the number of GFP⁺/CHX10⁺ cells in retinas electroporated with scrambled versus Dab1 shRNA. A highly significant decrease in GFP⁺/CHX10⁺ cells was observed upon Dab1-E knockdown (from 78% to 55%) (Fig. 9). The BrdU/CHX10 combined data indicate that both proliferation and the number of progenitor cells are decreased in retinas with reduced Dab1-E expression. Of note, we observed a general decrease in BrdU⁺ and CHX10⁺ cells in the vitreal half of the retina (Fig. 8 and 9).

We used the TUNEL (terminal deoxynucleotidyl transferase dUTP nick end labeling) assay and anti-pH 3 antibody labeling to demonstrate that neither apoptosis nor mitosis was affected by Dab1-E knockdown in the developing retina (see Fig. S6 in the supplemental material) (data not shown).

Knockdown of Dab1-E in the developing retina promotes ganglion cell differentiation. If Dab1-E knockdown affects cell proliferation, might it also affect retinal cell fate? To address this question, we first examined the number of early-born retinal neurons, ganglion and amacrine cells, in the GFP⁺ regions of ED7 chick retinas electroporated with either Dab1 shRNA or the scrambled shRNA control. Similar numbers of ganglion cells (Islet-1⁺) were observed in scrambled versus Dab1-E knockdown retinas (Fig. 10A). However, there appeared to be comparatively more GFP⁺ cells in the GCL of Dab1-E knockdown retinas than in scrambled retinas. To specifically measure the percentage of GFP⁺ cells expressing Islet-1 in scrambled versus Dab1-E knockdown cells, we first screened for retinas that had GFP expression in the same differentiation zone (the intermediate zone in the ventral retina was selected for our analyses). These matched retinas were then dissociated and coimmunostained with anti-GFP antibody and either anti-Islet-1 (ganglion marker) or AP-2 α (3B5; amacrine marker) antibody. A significant increase in the percentage of Islet-1⁺ GFP⁺ cells was observed in Dab1-E knockdown retinas (~3%) compared to that in scrambled controls (~1.7%) (Fig. 10B). Although we also observed more AP-2 α ⁺ GFP⁺ cells in

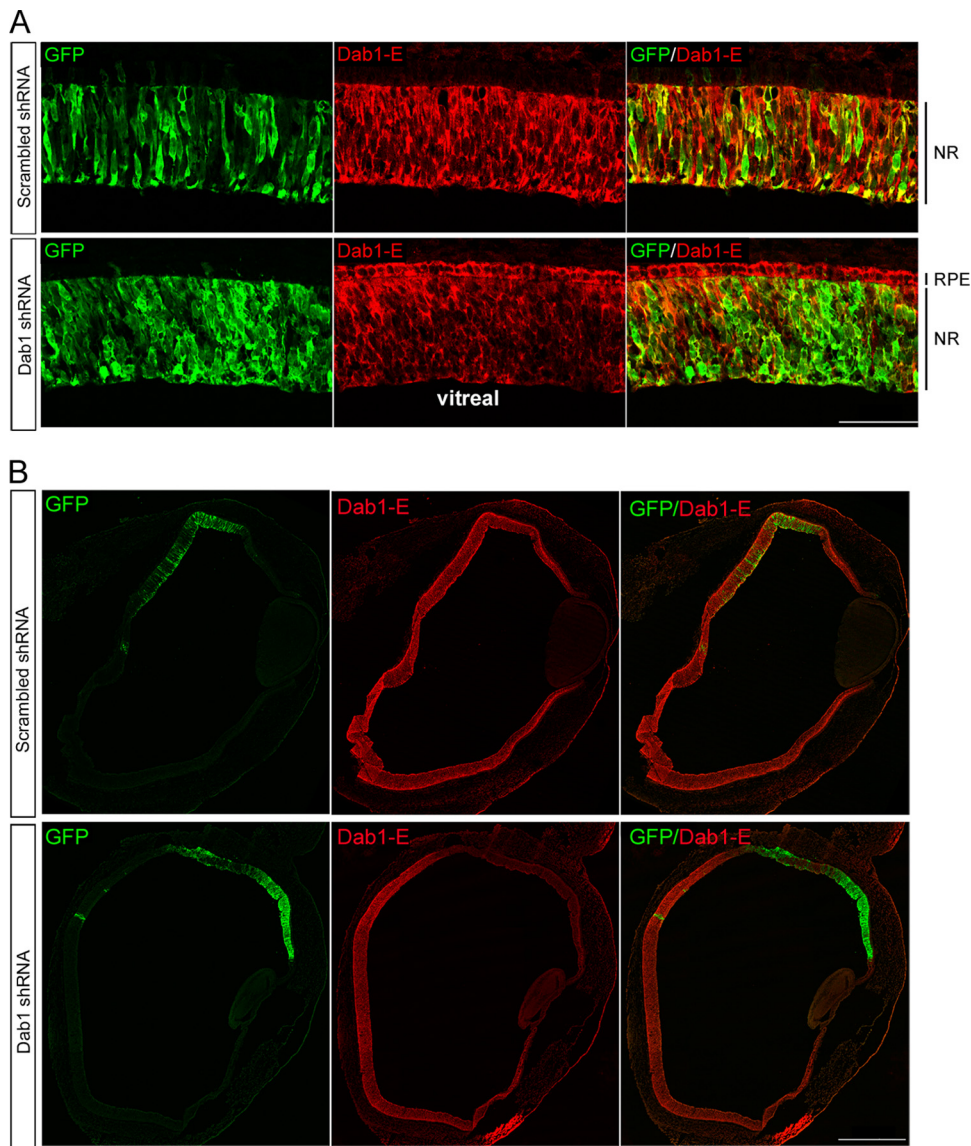


FIG. 7. Knockdown of Dab1-E in the developing chick retina. (A) Knockdown of Dab-E in ED5 chick retina. Cryosections from ED5 chick retinas electroporated with RCAS-GFP-Scrambled or RCAS-GFP-Dab1 shRNA were coimmunostained with goat anti-GFP and rabbit anti-Dab1-E antibodies. (B) Knockdown of Dab1-E in ED7 chick retina. Cryosections from ED7 chick retinas electroporated with RCAS-GFP-scrambled or RCAS-GFP-Dab1 shRNA were doubly immunostained with goat anti-GFP and rabbit anti-Dab1-E antibodies. Micrographs were collected with a Zeiss LSM 510 confocal microscope equipped with a 40 \times (A) or 10 \times (B) lens. A 3 \times 3 tile scan was applied to cover the entire retina in panel B. Abbreviations: RPE, retinal pigmented epithelium; NR, neural retina. Scale bar, 50 μ m (A) or 500 μ m (B).

Dab1-E knockdown retinas than in the control, this difference was not statistically significant (see Fig. S5 in the supplemental material).

γ -Secretase inhibition promotes conversion of Dab1-E to Dab1-L. Both Sonic Hedgehog (SHH) and Notch signaling have been shown to regulate retinal progenitor proliferation and neuronal cell fate in embryonic vertebrate retina (28, 61). To examine whether SHH and Notch can function through Dab1-E, we treated primary retinal cultures with either the SHH inhibitor cyclopamine or the γ -secretase inhibitor DAPT. The latter also inhibits Notch signaling. A significant decrease in Dab1-E transcripts, accompanied by a concomitant increase in Dab1-L transcripts, was observed upon treatment with

DAPT but not upon cyclopamine treatment (Fig. 11). These data suggest that Dab1 alternative splicing may be regulated by γ -secretase-controlled protein cleavages and that inhibition of γ -secretase, possibly through the inhibition of Notch signaling, promotes an isoform switch from Dab1-E to Dab1-L.

DISCUSSION

Alternative splicing is key to functional diversification of proteins in higher eukaryotes. Alternatively spliced Dab1 products have been documented in mouse, zebrafish, lizard, fruit fly, and chicken (6, 16, 23, 33, 42). However, other than a well-characterized role for Dab1 (Dab1-L) in Reelin-mediated

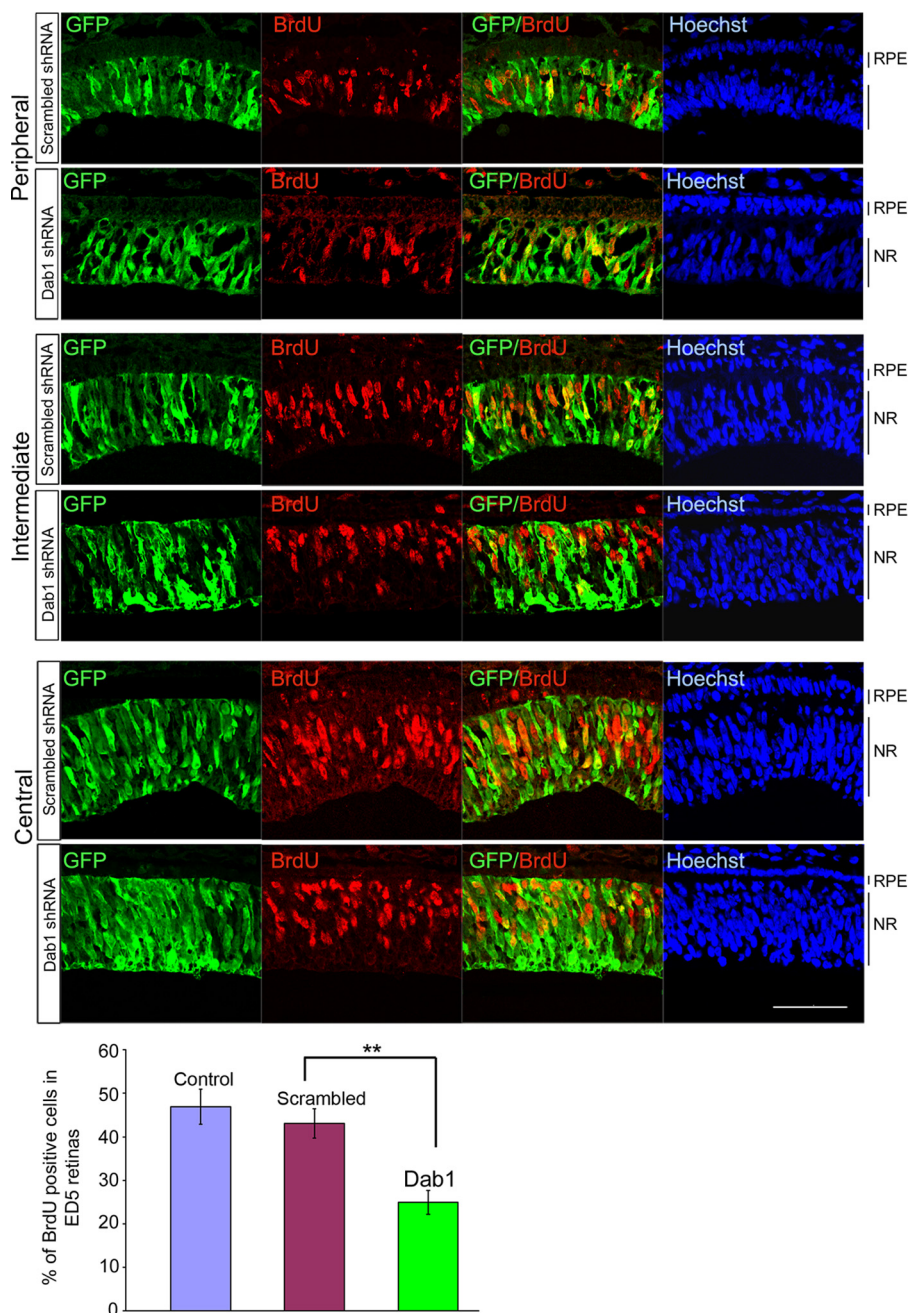


FIG. 8. BrdU incorporation in ED5 chick retinas electroporated with scrambled or Dab1 shRNA. BrdU and GFP were visualized by immunostaining with anti-mouse BrdU (1:100) and anti-goat GFP (1:2,000) antibodies. Sections were counterstained with Hoechst 33342 to label the nuclei. Representative images from peripheral, intermediate, and central zones from *in ovo* electroporated ED5 chick retinas are shown. Micrographs were collected with a Zeiss LSM 510 confocal microscope equipped with a 40 \times lens. Scale bar, 50 μ m. The histogram shows the percentage of GFP⁺ cells that are positive for BrdU. Values were derived from 6 controls and 6 scrambled and 8 Dab1 knockdown embryos. No significant difference was found between the control and scrambled groups. There was a significant difference between the scrambled and Dab1-E knockdown groups. **, $P < 0.01$ (t test). Abbreviations: RPE, retinal pigmented epithelium; NR, neural retina.

neuronal cell migration, the function of the other Dab1 isoforms remains poorly understood. Here we have shown that a form of Dab1 expressed at early stages of retinal development (Dab1-E) plays an important role in retinal neurogenesis. Of note, Dab1-E appears to function independently of Reelin-mediated tyrosine phosphorylation, revealing a novel aspect to Dab1 signaling.

Dab1-L function in the retina. In keeping with the observation that Dab1 is expressed in the IPL and AII amacrine cells of P7 and adult mouse retina (52), we found the highest levels of Dab1-L in the IPL of the chick retina, with a layering pattern similar to that found in mouse. However, two important differences were noted: (i) in contrast to mouse Dab1, chicken Dab1-L is not restricted to the amacrine lineage,

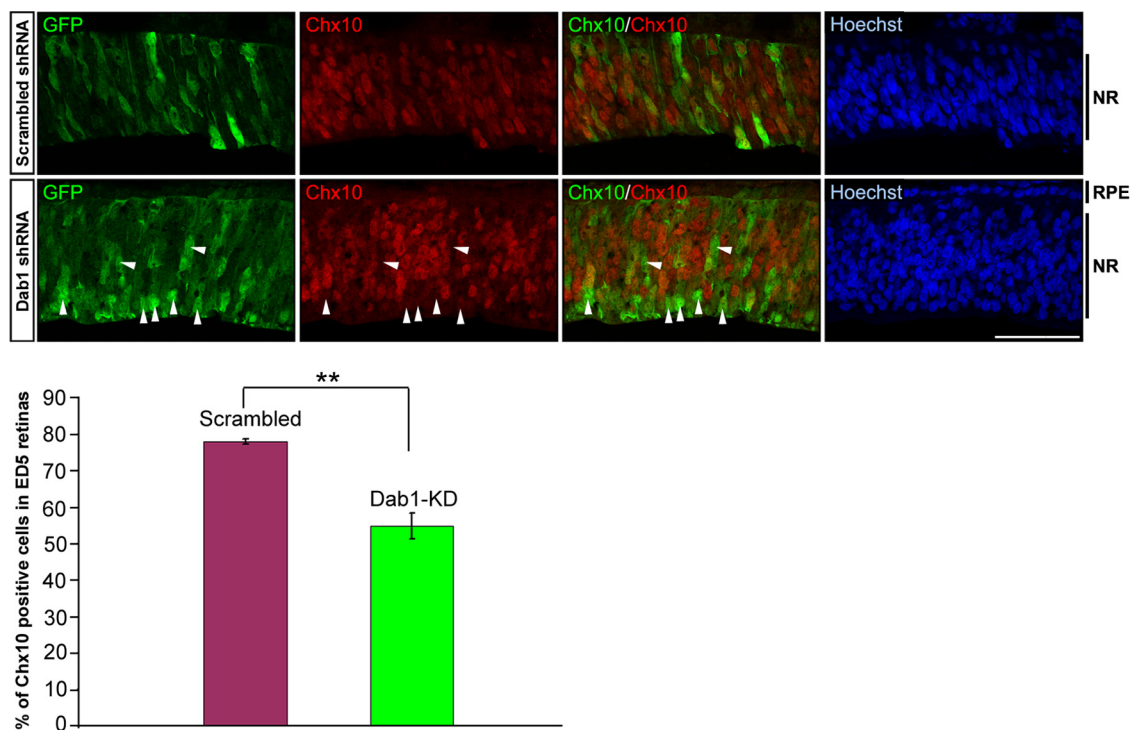


FIG. 9. Chx10 expression in ED5 chick retinas electroporated with scrambled or Dab1 shRNA. Chx10 and GFP were visualized by immunostaining with anti-sheep Chx10 (1:3,000) and anti-rabbit GFP (1:4,000) antibodies. Sections were counterstained with Hoechst 33342 to label the nuclei. Micrographs were collected from 4 eyes electroporated with scrambled shRNA and 4 eyes electroporated with Dab1 shRNA as described in the legend for Fig. 8. The arrows point to some of the GFP⁺ Chx10⁻ cells observed upon electroporation with Dab1 shRNA. Scale bar, 50 μ m. The histogram shows the percentage of GFP⁺ retinal cells that are positive for Chx10. There was a significant difference between the scrambled and Dab1-E knockdown groups. **, $P < 0.01$ (t test). Abbreviations: RPE, retinal pigmented epithelium; NBL, neuroblastic layer; GCL, ganglion cell layer.

and (ii) peaks of Dab1-L expression in chick retina correspond to peaks of neuronal differentiation, with elevated levels of Dab1-L sequentially observed in ganglion (ED5 to ED7), amacrine (ED8 to ED11), and horizontal (ED15 to P1) cells. These discrepancies can be partly explained by the fact that mouse retinas were only examined postnatally.

Although horizontal cells become postmitotic before amacrine cells (40, 51), they retain the ability to divide until relatively late stages of development (12). Furthermore, in contrast to other retinal cells, which directly reach their correct destination by somal translocation (7), horizontal cells show an unusual bidirectional migratory behavior, bypassing their correct layer before changing directions and migrating to their final destination (20). Thus, expression of Dab1-L in horizontal cells may be required for cell migration as well as for the formation of processes and/or synapses.

Dab1-E function in the retina. Dab1-E is widely expressed in proliferating retinal cells and in newly committed cells. Knockdown of Dab1-E at early stages of retinal development results in a significant decrease in proliferating cells, accompanied by a concomitant increase in ganglion cells. Dab1-E lacks two SFK tyrosine phosphorylation sites (Y198 and Y220) implicated in Reelin signaling but retains two Abl tyrosine phosphorylation sites (converted Y185 and Y232) and an intact PI/PTB domain, giving rise to the possibility that Dab1-E can bind Reelin receptors and function through Reelin. Importantly, our data indicate that Dab1-E plays a role that is inde-

pendent of Reelin-mediated tyrosine phosphorylation in the retina. First, endogenous Dab1-L but not Dab1-E is tyrosine phosphorylated in the retina. Second, exogenous Reelin induces Dab1-L but not Dab1-E tyrosine phosphorylation in primary retinal cultures. Third, we observed an excellent correlation between the temporal expression patterns of Reelin, Reelin receptor ApoER2, and Dab1-L but not Dab1-E in the developing retina. Although VLDLR is generally more abundant at later stages of retinal development, it should be noted that our attempts at immunostaining of retina tissue sections with anti-VLDLR antibody were not successful, leaving open the possibility that VLDLR may colocalize and interact with Dab1-E in the early retina. One possibility is that Dab1-E can compete with Dab1-L for binding to Reelin receptors and plays a dominant-negative role in Reelin signaling. Importantly, Dab1-E does not associate with CrkL (and likely CrkII, based on the similarity of their SH2 domains). Thus, Dab1-E appears unable to transmit Reelin-initiated signaling to well-established downstream effectors of this pathway.

A number of proteins other than Reelin receptors bind the Dab1 PI/PTB domain, including amyloid precursor proteins and Notch (24, 32, 45). Notch is of particular interest, since it is preferentially expressed in retinal progenitor cells and regulates progenitor cell competence by preventing premature cell cycle exit and differentiation of progenitor cells (18, 28). Importantly, inhibition of Notch signaling in the chick retina mimics the Dab1-E knockdown phenotype, particularly in re-

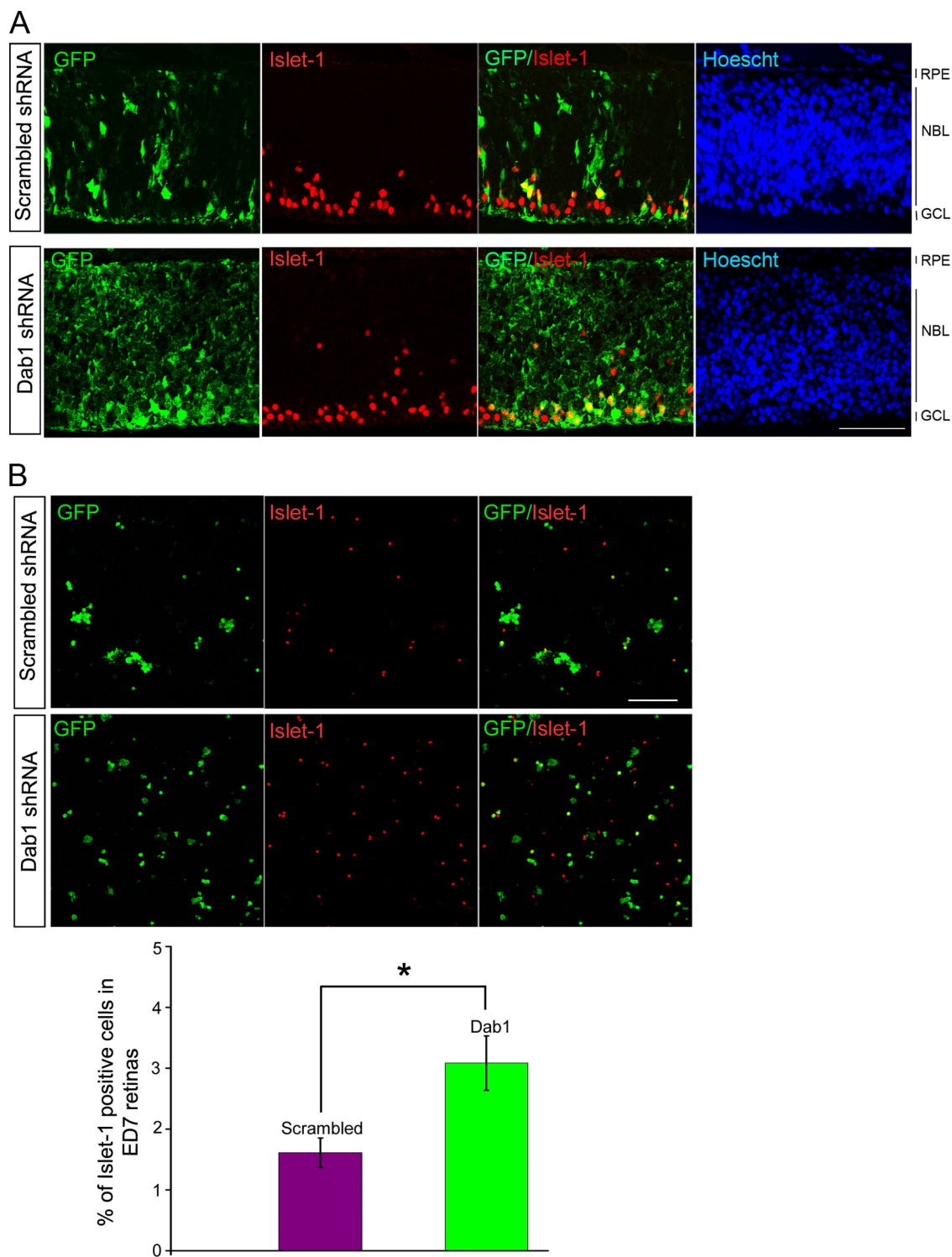


FIG. 10. Knockdown of Dab1 in chick retina promotes ganglion cell differentiation. (A) Coimmunostaining of Islet-1 and GFP in ED7 chick retinas electroporated with scrambled or Dab1 shRNA. Islet-1 and GFP were visualized by immunostaining with anti-mouse Islet-1 (1:1,500) and anti-goat GFP antibodies. Sections were counterstained with Hoechst 33342 to label the nuclei. Representative images from *in ovo*-electroporated ED7 chick retinas are shown. Micrographs were collected with a Zeiss LSM 510 confocal microscope equipped with a 40 \times lens. Scale bar, 50 μ m. (B) Analysis of Islet-1-positive cells in dissociated cells from ED7 chick retinas electroporated with scrambled or Dab1 shRNA. Dissociated retinal cells were coimmunostained with anti-mouse Islet-1 and anti-goat GFP, followed by donkey anti-mouse or donkey anti-goat secondary antibodies conjugated with Alexa 555 and Alexa 488, respectively. Micrographs were collected with a Zeiss LSM 510 confocal microscope equipped with a 20 \times lens in a tile scan mode (3 \times 3). Scale bar, 100 μ m. The bottom panel shows the quantitative analysis of electroporated/infected retinal cells positive for both GFP and Islet-1. Values were derived from 3 scrambled and 3 Dab1 knockdown embryos. There was a significant difference between the scrambled and Dab1-E knockdown groups. *, $P < 0.05$ (*t* test). Abbreviations: RPE, retinal pigmented epithelium; NBL, neuroblastic layer; GCL, ganglion cell layer.

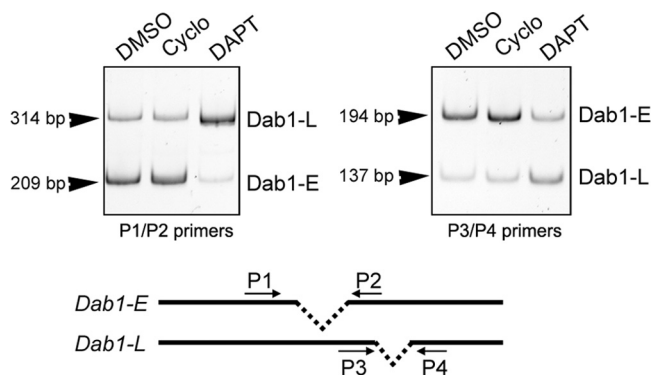


FIG. 11. RT-PCR analysis of Dab1-E and Dab1-L in ED5.5 retinal cells treated with DMSO, cyclopamine, and DAPT. cDNAs from ED5.5 retinal cells with indicated treatments were amplified using the primer set P1/P2 or P3/P4 (top panel). Sizes of amplified bands are indicated. Relative locations of primers in Dab1 transcripts are shown (bottom panel). Cyclo, cyclopamine.

lation to elevated ganglion cell differentiation (4). Furthermore, recent studies have shown that Dab1 enhances Notch signaling, likely by regulating the trafficking of the Notch intracellular domain (NICD) to prevent its degradation (27). This raises the possibility that Dab1-E may maintain the retinal progenitor pool by controlling NICD trafficking.

Is Dab1-E specific to the chicken? Our data suggest a role for Dab1-E in the maintenance of the chick retina progenitor pool that is independent of Reelin-mediated tyrosine phosphorylation. Although Dab1-E-like isoforms have been detected in mice and other species by RT-PCR and *in situ* hybridization (6, 16), it is not clear what role, if any, these isoforms play in these species. Dab1 555*, which contains the Dab1-E-specific insertion region, is expressed in the ventricular zone of the mouse cerebral cortex at ED14, at the peak of neurogenesis (6). In addition, knock-in of a Dab1 allele missing the two consensus SFK phosphorylation sites (Y185 and Y198) in mice, effectively mimicking Dab1-E, results in a milder phenotype in the cortex, hippocampus, and cerebellum than that for Dab1 knockout mice (22). The Y185/Y198 mutant Dab1 protein shows little or no response to Reelin and does not recruit SFKs, in support of a Reelin-independent Dab1 function.

A number of factors may explain why Reelin-independent Dab1-E has not been detected in other species to date. First, the Dab1 B3 antibody, documented here to specifically recognize Dab1-L, has commonly been used to detect Dab1 expression in mice. Directly relevant to our study, Dab1 B3 antibody was used to examine Dab1 expression in mouse retina (52–53). Murine Dab1-E-like isoforms may have been missed using this antibody. Second, Bar et al. (6) used only primers/probes specific to the insertion region of Dab1-E in their search for Dab1 isoforms in mice, humans, and other species. Primers/probes spanning both the deletion and insertion regions may reveal the presence of Dab1-E in these species. Third, whereas the insertion in chicken Dab1-E spans 19 aa, the insertion in putative mammalian Dab1-E (based on RT-PCR analysis) is 33 aa due to exon duplication. Thus, the difference in size between mammalian Dab1-L and the predicted mammalian Dab1-E is only 2 amino acids, making it difficult to distinguish these two forms based on Northern and Western blots. Fourth,

as shown here, Dab1-E is expressed primarily at early stages of development and consequently may have been missed in studies concentrating on later stages. Finally, a compelling reason not to invoke the need for a Reelin-independent isoform has been the similarity in the phenotypes reported for Reelin and Dab1 mutant mice, suggesting that all Dab1 functions are mediated through Reelin (34, 55). However, some differences have been noted between *Dab1*-deficient mice and *reeler* mice. For example, the number of Purkinje cells is higher in the cerebellum of *scrambler* mice than in those of *reeler* mice, and chain formation defects in the rostral migratory stream have been observed in *Dab1*^{-/-} mice but not in *reeler* mice (2, 25). A detailed analysis of the phenotypes resulting from Reelin and Dab1 knockout may reveal additional differences.

In summary, we present evidence that developmentally regulated alternative splicing of the *Dab1* gene gives rise to two key functional isoforms in the chick retina: Dab1-E, which is expressed in retinal progenitor cells and plays a role in maintaining the retinal progenitor pool at early developmental stages, and Dab1-L, which is expressed in differentiated retinal cells and is likely involved in the formation of dendrites/axons and synaptic connections. We propose that phenotypes traditionally associated with Dab1 depletion or knockout may actually represent an amalgamation of Dab1-E and Dab1-L loss of function. Future studies characterizing the molecular mechanisms underlying Dab1 alternative splicing will be instrumental in understanding this precisely timed, developmentally regulated process.

ACKNOWLEDGMENTS

We are grateful to Jonathan A. Cooper for the anti-Dab1 (B3) antibody, Tom Curran for the pCrI-Reelin construct, Joachim Herz for the ApoER2 antibody, and Jianxun Han for the γ -secretase inhibitor DAPT. We thank Xuejun Sun and Gerry Barron for their help with cell scoring using the Metamorph software program.

This work was supported by the Canadian Institutes of Health Research. Z.G. is supported by an Alberta Heritage Foundation for Medical Research studentship and a Dissertation Fellowship from the University of Alberta.

REFERENCES

- Altshuler, D., and C. Cepko. 1992. A temporally regulated, diffusible activity is required for rod photoreceptor development in vitro. *Development* **114**: 947–957.
- Andrade, N., V. Komnenovic, S. M. Blake, Y. Jossin, B. Howell, A. Goffinet, W. J. Schneider, and J. Nimpf. 2007. ApoER2/VLDL receptor and Dab1 in the rostral migratory stream function in postnatal neuronal migration independently of Reelin. *Proc. Natl. Acad. Sci. U. S. A.* **104**:8508–8513.
- Arnaud, L., B. A. Ballif, E. Forster, and J. A. Cooper. 2003. Fyn tyrosine kinase is a critical regulator of disabled-1 during brain development. *Curr. Biol.* **13**:9–17.
- Austin, C. P., D. E. Feldman, J. A. Ida, Jr., and C. L. Cepko. 1995. Vertebrate retinal ganglion cells are selected from competent progenitors by the action of Notch. *Development* **121**:3637–3650.
- Ballif, B. A., L. Arnaud, W. T. Arthur, D. Guris, A. Imamoto, and J. A. Cooper. 2004. Activation of a Dab1/CrkL/C3G/Rap1 pathway in Reelin-stimulated neurons. *Curr. Biol.* **14**:606–610.
- Bar, I., F. Tissir, C. Lambert de Rouvroit, O. De Backer, and A. M. Goffinet. 2003. The gene encoding disabled-1 (DAB1), the intracellular adaptor of the Reelin pathway, reveals unusual complexity in human and mouse. *J. Biol. Chem.* **278**:5802–5812.
- Baye, L. M., and B. A. Link. 2008. Nuclear migration during retinal development. *Brain Res.* **1192**:29–36.
- Belecky-Adams, T., S. Tomarev, H. S. Li, L. Ploder, R. R. McInnes, O. Sundin, and R. Adler. 1997. Pax-6, Prox 1, and Chx10 homeobox gene expression correlates with phenotypic fate of retinal precursor cells. *Invest. Ophthalmol. Vis. Sci.* **38**:1293–1303.
- Bernier, B., I. Bar, G. D'Arcangelo, T. Curran, and A. M. Goffinet. 2000. Reelin mRNA expression during embryonic brain development in the chick. *J. Comp. Neurol.* **422**:448–463.

10. **Bock, H. H., and J. Herz.** 2003. Reelin activates SRC family tyrosine kinases in neurons. *Curr. Biol.* **13**:18–26.
11. **Bock, H. H., Y. Jossin, P. Liu, E. Forster, P. May, A. M. Goffinet, and J. Herz.** 2003. Phosphatidylinositol 3-kinase interacts with the adaptor protein Dab1 in response to Reelin signaling and is required for normal cortical lamination. *J. Biol. Chem.* **278**:38772–38779.
12. **Boije, H., P. H. Edqvist, and F. Hallbook.** 2009. Horizontal cell progenitors arrest in G2-phase and undergo terminal mitosis on the vitreal side of the chick retina. *Dev. Biol.* **330**:105–113.
13. **Cepko, C. L., C. P. Austin, X. Yang, M. Alexiades, and D. Ezzeddine.** 1996. Cell fate determination in the vertebrate retina. *Proc. Natl. Acad. Sci. U. S. A.* **93**:589–595.
14. **Chai, X., E. Forster, S. Zhao, H. H. Bock, and M. Frotscher.** 2009. Reelin stabilizes the actin cytoskeleton of neuronal processes by inducing n-cofilin phosphorylation at serine3. *J. Neurosci.* **29**:288–299.
15. **Chen, K., P. G. Ochalski, T. S. Tran, N. Sahir, M. Schubert, A. Pramatarova, and B. W. Howell.** 2004. Interaction between Dab1 and CrkII is promoted by Reelin signaling. *J. Cell Sci.* **117**:4527–4536.
16. **Costagli, A., B. Felice, A. Guffanti, S. W. Wilson, and M. Mione.** 2006. Identification of alternatively spliced dab1 isoforms in zebrafish. *Dev. Genes Evol.* **216**:291–299.
17. **D'Arcangelo, G., G. G. Miao, S. C. Chen, H. D. Soares, J. I. Morgan, and T. Curran.** 1995. A protein related to extracellular matrix proteins deleted in the mouse mutant reeler. *Nature* **374**:719–723.
18. **Del Bene, F., A. M. Wehman, B. A. Link, and H. Baier.** 2008. Regulation of neurogenesis by interkinetic nuclear migration through an apical-basal notch gradient. *Cell* **134**:1055–1065.
19. **Dutting, D., A. Gierer, and G. Hansmann.** 1983. Self-renewal of stem cells and differentiation of nerve cells in the developing chick retina. *Brain Res.* **312**:21–32.
20. **Edqvist, P. H., and F. Hallbook.** 2004. Newborn horizontal cells migrate bi-directionally across the neuroepithelium during retinal development. *Development* **131**:1343–1351.
21. **Federspiel, M. J., and S. H. Hughes.** 1997. Retroviral gene delivery. *Methods Cell Biol.* **52**:179–214.
22. **Feng, L., and J. A. Cooper.** 2009. Dual functions of Dab1 during brain development. *Mol. Cell Biol.* **29**:324–332.
23. **Gertler, F. B., K. K. Hill, M. J. Clark, and F. M. Hoffmann.** 1993. Dosage-sensitive modifiers of *Drosophila* abl tyrosine kinase function: prospero, a regulator of axonal outgrowth, and disabled, a novel tyrosine kinase substrate. *Genes Dev.* **7**:441–453.
24. **Giniger, E.** 1998. A role for Abl in Notch signaling. *Neuron* **20**:667–681.
25. **Goldowitz, D., R. C. Cushing, E. Laywell, G. D'Arcangelo, M. Sheldon, H. O. Sweet, M. Davisson, D. Steindler, and T. Curran.** 1997. Cerebellar disorganization characteristic of reeler in scrambler mutant mice despite presence of reelin. *J. Neurosci.* **17**:8767–8777.
26. **Hamburger, V., and H. L. Hamilton.** 1951. A series of normal stages in the development of the chick embryo. *J. Morphol.* **88**:49–92.
27. **Hashimoto-Torii, K., M. Torii, M. R. Sarkisian, C. M. Bartley, J. Shen, F. Radtke, T. Gridley, N. Sestan, and P. Rakic.** 2008. Interaction between Reelin and Notch signaling regulates neuronal migration in the cerebral cortex. *Neuron* **60**:273–284.
28. **Horrique, D., E. Hirsinger, J. Adam, I. Le Roux, O. Pourquie, D. Ish-Horowicz, and J. Lewis.** 1997. Maintenance of neuroepithelial progenitor cells by Delta-Notch signalling in the embryonic chick retina. *Curr. Biol.* **7**:661–670.
29. **Herrick, T. M., and J. A. Cooper.** 2002. A hypomorphic allele of dab1 reveals regional differences in reelin-Dab1 signaling during brain development. *Development* **129**:787–796.
30. **Hiesberger, T., M. Trommsdorff, B. W. Howell, A. Goffinet, M. C. Mumby, J. A. Cooper, and J. Herz.** 1999. Direct binding of Reelin to VLDL receptor and ApoE receptor 2 induces tyrosine phosphorylation of disabled-1 and modulates tau phosphorylation. *Neuron* **24**:481–489.
31. **Holt, C. E., T. W. Bertsch, H. M. Ellis, and W. A. Harris.** 1988. Cellular determination in the *Xenopus* retina is independent of lineage and birth date. *Neuron* **1**:15–26.
32. **Homayouni, R., D. S. Rice, M. Sheldon, and T. Curran.** 1999. Disabled-1 binds to the cytoplasmic domain of amyloid precursor-like protein 1. *J. Neurosci.* **19**:7507–7515.
33. **Howell, B. W., F. B. Gertler, and J. A. Cooper.** 1997. Mouse disabled (mDab1): a Src binding protein implicated in neuronal development. *EMBO J.* **16**:121–132.
34. **Howell, B. W., R. Hawkes, P. Soriano, and J. A. Cooper.** 1997. Neuronal position in the developing brain is regulated by mouse disabled-1. *Nature* **389**:733–737.
35. **Howell, B. W., T. M. Herrick, and J. A. Cooper.** 1999. Reelin-induced tyrosine phosphorylation of disabled 1 during neuronal positioning. *Genes Dev.* **13**:643–648.
36. **Howell, B. W., T. M. Herrick, J. D. Hildebrand, Y. Zhang, and J. A. Cooper.** 2000. Dab1 tyrosine phosphorylation sites relay positional signals during mouse brain development. *Curr. Biol.* **10**:877–885.
37. **Hughes, S. H., J. J. Greenhouse, C. J. Petropoulos, and P. Suttrave.** 1987. Adaptor plasmids simplify the insertion of foreign DNA into helper-independent retroviral vectors. *J. Virol.* **61**:3004–3012.
38. **Iijima, H., M. Miyazawa, J. Sakai, K. Magoori, M. R. Ito, H. Suzuki, M. Nose, Y. Kawarabayasi, and T. T. Yamamoto.** 1998. Expression and characterization of a very low density lipoprotein receptor variant lacking the O-linked sugar region generated by alternative splicing. *J. Biochem.* **124**:747–755.
39. **Jossin, Y., and A. M. Goffinet.** 2007. Reelin signals through phosphatidylinositol 3-kinase and Akt to control cortical development and through mTOR to regulate dendritic growth. *Mol. Cell Biol.* **27**:7113–7124.
40. **Kahn, A. J.** 1974. An autoradiographic analysis of the time of appearance of neurons in the developing chick neural retina. *Dev. Biol.* **38**:30–40.
41. **Katyal, S., Z. Gao, E. Monckton, D. Glubrecht, and R. Godbout.** 2007. Hierarchical disabled-1 tyrosine phosphorylation in Src family kinase activation and neurite formation. *J. Mol. Biol.* **368**:349–364.
42. **Katyal, S., and R. Godbout.** 2004. Alternative splicing modulates Disabled-1 (Dab1) function in the developing chick retina. *EMBO J.* **23**:1878–1888.
43. **Keshvara, L., D. Benhayon, S. Magdaleno, and T. Curran.** 2001. Identification of reelin-induced sites of tyrosyl phosphorylation on disabled 1. *J. Biol. Chem.* **276**:16008–16014.
44. **Lambert de Rouvroit, C., V. de Bergeyck, C. Cortvrindt, I. Bar, Y. Eeckhout, and A. M. Goffinet.** 1999. Reelin, the extracellular matrix protein deficient in reeler mutant mice, is processed by a metalloproteinase. *Exp. Neurol.* **156**:214–217.
45. **Le Gall, M., C. De Mattei, and E. Giniger.** 2008. Molecular separation of two signaling pathways for the receptor, Notch. *Dev. Biol.* **313**:556–567.
46. **Le, N., and M. A. Simon.** 1998. Disabled is a putative adaptor protein that functions during signaling by the sevenless receptor tyrosine kinase. *Mol. Cell Biol.* **18**:4844–4854.
47. **Li, X., D. D. Glubrecht, R. Mita, and R. Godbout.** 2008. Expression of AP-2delta in the developing chick retina. *Dev. Dyn.* **237**:3210–3221.
48. **Nabi, N. U., E. Mezer, S. I. Blaser, A. A. Levin, and J. R. Buncic.** 2003. Ocular findings in lissencephaly. *J. AAPOS* **7**:178–184.
49. **Park, T. J., and T. Curran.** 2008. Crk and Crk-like play essential overlapping roles downstream of Disabled-1 in the Reelin pathway. *J. Neurosci.* **28**:13551–13562.
50. **Prada, C., J. Puga, L. Perez-Mendez, R. Lopez, and G. Ramirez.** 1991. Spatial and temporal patterns of neurogenesis in the chick retina. *Eur. J. Neurosci.* **3**:559–569.
51. **Reh, T. A., and I. J. Kljavin.** 1989. Age of differentiation determines rat retinal germinal cell phenotype: induction of differentiation by dissociation. *J. Neurosci.* **9**:4179–4189.
52. **Rice, D. S., and T. Curran.** 2000. Disabled-1 is expressed in type AII amacrine cells in the mouse retina. *J. Comp. Neurol.* **424**:327–338.
53. **Rice, D. S., S. Nusinowitz, A. M. Azimi, A. Martinez, E. Soriano, and T. Curran.** 2001. The Reelin pathway modulates the structure and function of retinal synaptic circuitry. *Neuron* **31**:929–941.
54. **Schiffmann, S. N., B. Bernier, and A. M. Goffinet.** 1997. Reelin mRNA expression during mouse brain development. *Eur. J. Neurosci.* **9**:1055–1071.
55. **Sheldon, M., D. S. Rice, G. D'Arcangelo, H. Yoneshima, K. Nakajima, K. Mikoshiba, B. W. Howell, J. A. Cooper, D. Goldowitz, and T. Curran.** 1997. Scrambler and yotari disrupt the disabled gene and produce a reeler-like phenotype in mice. *Nature* **389**:730–733.
56. **Songyang, Z., S. E. Shoelson, M. Chaudhuri, G. Gish, T. Pawson, W. G. Haser, F. King, T. Roberts, S. Ratnofsky, R. J. Lechleider, et al.** 1993. SH2 domains recognize specific phosphopeptide sequences. *Cell* **72**:767–778.
57. **Sun, X. M., and A. K. Soutar.** 1999. Expression in vitro of alternatively spliced variants of the messenger RNA for human apolipoprotein E receptor-2 identified in human tissues by ribonuclease protection assays. *Eur. J. Biochem.* **262**:230–239.
58. **Trommsdorff, M., J. P. Borg, B. Margolis, and J. Herz.** 1998. Interaction of cytosolic adaptor proteins with neuronal apolipoprotein E receptors and the amyloid precursor protein. *J. Biol. Chem.* **273**:33556–33560.
59. **Trommsdorff, M., M. Gotthardt, T. Hiesberger, J. Shelton, W. Stockinger, J. Nimpf, R. E. Hammer, J. A. Richardson, and J. Herz.** 1999. Reeler/Disabled-like disruption of neuronal migration in knockout mice lacking the VLDL receptor and ApoE receptor 2. *Cell* **97**:689–701.
60. **Turner, D. L., and C. L. Cepko.** 1987. A common progenitor for neurons and glia persists in rat retina late in development. *Nature* **328**:131–136.
61. **Wang, Y., G. D. Dakubo, S. Thuring, C. J. Mazerolle, and V. A. Wallace.** 2005. Retinal ganglion cell-derived sonic hedgehog locally controls proliferation and the timing of RGC development in the embryonic mouse retina. *Development* **132**:5103–5113.